STUK-TR 1 / JUNE 2007

TR

Application of TONUS V2006 and FLUENT 6.2.16 CFD codes to ENACCEF hydrogen combustion tests

Eveliina Takasuo, Risto Huhtanen

Säteilyturvakeskus
Strålsäkerhetscentralen
Radiation and Nuclear Safety Authority

STUK

STUK-TR 1 / JUNE 2007

Application of TONUS V2006 and FLUENT 6.2.16 CFD codes to ENACCEF hydrogen combustion tests

Eveliina Takasuo, Risto Huhtanen

VTT

In STUK this study has been supervised by Risto Sairanen

STUK • **SÄTEILYTURVAKESKUS**
STRÅLSÄKERHETSCENTRALEN
RADIATION AND NUCLEAR SAFETY AUTHORITY

Osoite/Address • Laippatie 4, 00880 Helsinki
Postiosoite / Postal address • PL / P.O.Box 14, FIN-00881 Helsinki, FINLAND
Puh./Tel. (09) 759 881, +358 9 759 881 • Fax (09) 759 88 500, +358 9 759 88 500 • www.stuk.fi

The conclusions presented in the STUK report series are those of the authors and do not necessarily represent the official position of STUK.

ISBN 978-952-478-225-8 (print, Edita Prima Oy, Finland 2007)
ISBN 978-952-478-226-5 (pdf)
ISSN 1796-7171

TAKASUO Eveliina, HUHTANEN Risto. Application of TONUS V2006 and FLUENT 6.2.16 CFD codes to ENACCEF hydrogen combustion tests. STUK-TR 1. Helsinki 2007. 34 pp

Keywords: hydrogen deflagration, ENACCEF, TONUS, FLUENT, CRECBOM model, Eddy Break-up model

Abstract

Three ENACCEF hydrogen combustion tests have been simulated for code validation purposes using the TONUS V2006 and FLUENT 6.2.16 CFD software. The test series investigated deflagration in a uniform hydrogen concentration, in a concentration that decreases and in a concentration that increases along the height of the facility. In the TONUS calculations the CREBCOM combustion model and k-ε turbulence model with Eddy Break-Up (EBU) reaction kinetics have been used. In the FLUENT calculations only the k-ε and EBU models have been used and the simulation results are compared to each other and the test results.

TONUS CREBCOM results of the uniform mixture case obtained by 3D model of the facility are qualitatively in a reasonable agreement with the test results. In the increasing concentration case the flame speeds are exaggerated while in the decreasing concentration case the flame acceleration is underestimated. Further evaluation of the model parameters is suggested for non-homogenous mixtures. Generally, the EBU calculations by FLUENT show similar pressures and flame speed profiles with slightly higher maximum speeds as the CREBCOM cases. Also the FLUENT results are in a relatively good agreement with the test results.

Preface

This code validation work is conducted in order to assess the capabilities of the TONUS and FLUENT CFD software for Olkiluoto 3 hydrogen risk analysis. The TONUS code was acquired to VTT from CEA, France, within the framework of the SAFIR national research programme in 2006. The study is based on experimental data released as a specification for a benchmark exercise performed by the partners of the European Severe Accident Network of Excellence (SARNET) Workpackage 12.1. The first author wishes to thank Dr. Sergey Kudriakov, CEA Saclay, for valuable assistance in using the TONUS code.

Espoo, 19.4.2007

Eveliina Takasuo, Risto Huhtanen

Contents

Nomenclature

A	Constant in FLUENT EBU model
B	Constant in FLUENT EBU model
C_{EBU}	Eddy Break-Up constant in TONUS EBU model
$C_{\varepsilon 1}, C_{\varepsilon 2}, C_{\varepsilon 3}$	constants in the ε equation of the k-ε turbulence model
D_k	diffusion coefficient of species k into the gas mixture (m²/s)
e_{tot}	specific total energy (J/kg)
G	a buoyancy term in the equation for k and ε in the k-ε turbulence model (kg/m/s³)
$\vec{g}$	gravitational acceleration (m/s²)
h_{tot}	specific total enthalpy (J/kg)
K_0	parameter of the CREBCOM model related to the flame velocity (m/s)
k	turbulent kinetic energy (m²/s²)
L	integral length scale of turbulence (m)
Le	Lewis number
m_{H_2}	mass fraction of hydrogen in FLUENT model
m_{O_2}	mass fraction of oxygen in FLUENT model
m_{prod}	mass fraction of combustion products in FLUENT model
N	total number of species in the gas mixture
P	pressure (Pa)
$\vec{r}$	position vector (m)
$\vec{q}$	energy flux vector (J/m²/s)
P_k	a term in the equation for k and ε in the k-ε turbulence model (kg/m/s³)
R_{H_2}	kg/m³/s reaction rate of hydrogen combustion in FLUENT model
s_{O_2}	stoichiometric ratio of oxygen
s_{prod}	stoichiometric ratio of combustion products
S_{cr}	source term in the energy equation of the CREBCOM model (W/m³)
S_L	laminar burning rate (m/s)
S_T	turbulent burning rate (m/s)
t	time (s)
$\vec{u}$	flow velocity (m/s)
Y_k	mass fraction of the species k (k = 1,…,N)
$Y_{H2,i}$	hydrogen mass fraction in the unburnt mixture
$Y_{H2,f}$	hydrogen mass fraction in the burnt mixture

Greek symbols

δ	laminar flame thickness (m)
$\Delta h_{f,k}$	mass formation enthalpy of species k (J/kg)
Δx	dimension of the computational grid (m)
ε	rate of turbulent energy dissipation (m²/s³)
ε_{cr}	parameter in the criterion function of the CREBCOM model
μ	kg/m/s dynamic viscosity of the gas mixture
μ_t	kg/m/s dynamic viscosity of the gas mixture due to turbulence
ξ	progress variable in the CREBCOM model
ρ	kg/m³ density of the gas mixture
ρ_{H2}	kg/m³ density of the species k (k = 1,…,N)
τ^t	kg/m/s² turbulent viscous stress tensor
$\acute{\omega}$	mol/m³/s global reaction rate in TONUS models
$\acute{\omega}_k$	kg/m³/s reaction rate of species k (k=1,...,N) in TONUS models
σ	expansion ratio
σ_k	constant in the k-equation of the k-ε model
σ_ε	constant in the ε-equation of the k-ε model

Abbreviations

AIBC	Adiabatic IsoBaric complete Combustion
AICC	Adiabatic IsoChoric complete Combustion
CEA	Commissariat à l'Energie Atomique
CREBCOM	CRiteria and Experimentally Based COmbustion Model
DDT	Deflagration–to–detonation transition

1 Introduction

Hydrogen issues have been identified as important matters in recent containment safety analysis. In case hydrogen mitigation is not possible, or has at least partly failed, it is important to know the flame speeds and pressure rise if a combustible cloud containing hydrogen is ignited.

The TONUS CFD code is developed in France by IRSN and CEA for hydrogen distribution and combustion analysis especially for nuclear power plant safety applications. The code was acquired to VTT and a user-training period was provided by CEA in 2006 within the framework of the SAFIR programme. The code was introduced at VTT as a possible independent tool for hydrogen risk calculations for the needs of the Finnish nuclear power plants, especially Olkiluoto 3. The code must be validated for its designed purpose against experimental data from test facilities appropriate for predicting phenomena in full-scale containment geometries.

The ENACCEF facility is a hydrogen combustion test facility operated by CRSN and IRSN, France, and it was selected for the simulation because of its vertical flame propagation, possibility to install obstacles into the flow tube and larger upper volume. The facility is designed especially for investigating flame behaviour in non-uniform hydrogen-air mixtures. The three tests with different initial hydrogen concentrations presented by Bentaib [3] as a specification of a SARnet benchmark exercise are simulated in this study.

In addition to TONUS, the tests are modelled using the FLUENT 6.2.16 commercial CFD package and the results obtained by FLUENT are compared to the TONUS results. In the TONUS calculations, focus is on the CREBCOM combustion model and the selection of the model key parameter K_0 that determines the combustion rate in this simplified combustion model. Also the standard k-ε turbulence model with Eddy Break-Up reaction kinetics model has been tested. In the FLUENT calculation, only the k-ε model with EBU chemistry incorporated into the code is used.

2 Goal

The main goal of the study was to validate TONUS and FLUENT codes against the ENACCEF hydrogen combustion test. This report contains the descriptions and a short analytical comparison of the models used in the codes and analysis of the results given by the two codes against the experimental flame speed data.

3 Limitations

The present report focuses on the comparison of the simulation results obtained by the two codes, analysis of the computational methods used and methods for finding the key parameter K_0 of the CREBCOM model. At the moment, only the flame speed measurement data reported by Bentaib [3] is available of the test results. Thus, the comparisons of the test and simulation results are limited to the flame speeds though comparison of pressure data could provide a more detailed insight into the system behaviour and the performance of the codes.

The combustible gas mixture present in the tests is composed of hydrogen with varying concentrations and dry air. The effect of steam on flame propagation is not studied.

4 Test description

4.1 ENACCEF facility

The following description of the test facility is given in [3] and [10]. The ENACCEF facility consists of a 3.3 m-long stainless steel acceleration tube and a larger cylindrical dome volume whose top is at the height of 5.0 m. The inner diameter of the acceleration tube is 0.154 m and for the dome 0.738 m. The schematic of the facility is presented in Figure 1. The acceleration tube is equipped with two tungsten electrodes at 0.138 m from the bottom of the facility as a low-energy ignition device. The ignition energy is approximately 600 mJ.

In the tests nine annular obstacles, of the type shown in Figure 2, were installed into the acceleration tube, starting from 0.638 m from the point of ignition. The distance between the obstacles is 0.154 m and they provide a blockage ratio of 0.63.

The instrumentation of the facility consists of 16 UV-sensitive photomultipliers mounted across silica windows located along the acceleration tube and the dome wall and nine pressure transducers (7 PZT and 2 PCB transducers) as shown in Figure 1b, one of which is attached on the inner top wall of the dome to monitor pressure build-up during a test. Gas sampling is performed at six different locations in the acceleration tube and one in the dome.

a)

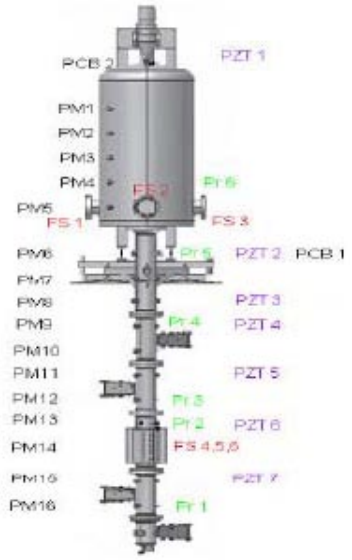

b)

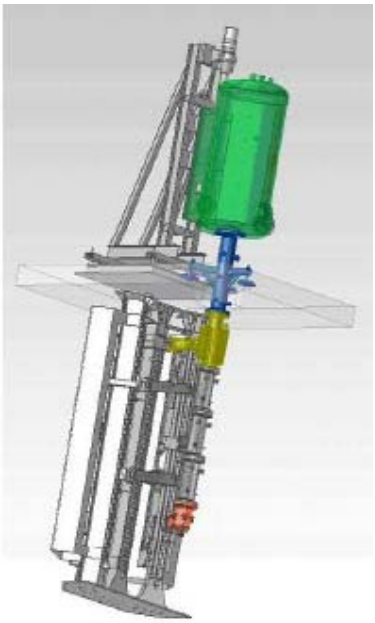

Figure 1. The ENACCEF facility. **a)** Side view with the approximate measurement locations [3]. **(b)** Schematic of the test arrangement [10].

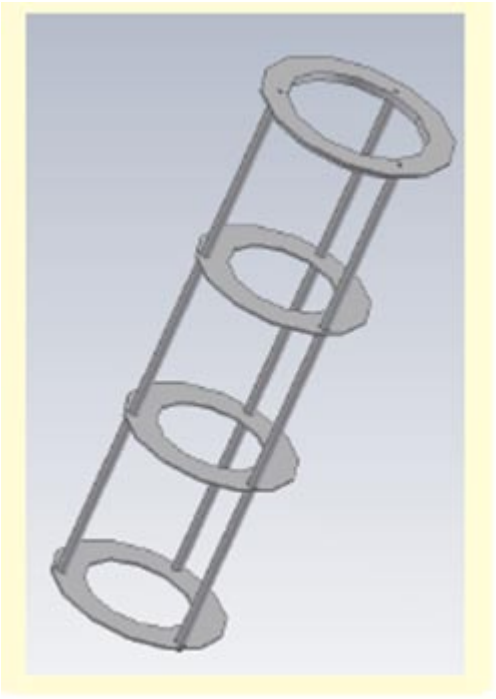

Figure 2. Annular obstacles installed into the acceleration tube [3].

4.2 Test procedures

Prior to the tests, the facility is vacuumed down below 1 Pa and hydrogen-air mixture of desired composition is introduced via flow meter controllers. The mixture is composed of dry compressed air and hydrogen with purity better than 99.95% [3].

4.2.1 Uniform hydrogen concentration

In this test, the facility was filled with premixed gas composed of 13% hydrogen and 87% of air via injection from the bottom and top parts of the facility until 100 kPa pressure was reached. The homogenous mixture with the volume fraction of 13% hydrogen is ignited at 0.138 m from the acceleration tube bottom.

4.2.2 Negative and positive hydrogen concentration gradients

In these two tests the initial hydrogen concentration varies according to the vertical position in the acceleration tube. The negative gradient, where the hydrogen fraction is reduced towards the top of the acceleration tube, is achieved by, at first, filling the facility with a premixed gas composed of 10.5% hydrogen, 89.5% dry air up to 99.725 kPa. Then, pure hydrogen is injected during two minutes into the bottom of the facility with a rate of 0.5 l/min. After about 5 minutes, gas sampling is performed and the mixture is ignited.

Table 1. Mixture composition during injection in the positive gradient experiment.

Time	Vol. fraction of H_2	Vol. fraction of air
0–180 s	13 %	87 %
181–300 s	12 %	88 %
301–420 s	11 %	89 %
421–541 s	10.5 %	89.5 %

The positive gradient is achieved by filling the facility with gas mixture which contains 13% hydrogen and 87% air up to 89.325 Pa. Then hydrogen-air mixture is injected into the bottom of the facility during 9 minutes with a rate of 7.2 l/min and with the concentration given in Table 1.

During the pressurization the dome and the acceleration tube are separated by a terphane membrane and the dome volume is filled simultaneously with the tube. The mean molar fractions of hydrogen in the acceleration tube obtained in the test series are presented in Figure 3 which includes also the linear approximations of the curves. These linear approximations are used to determine the initial hydrogen fractions in the TONUS calculation. In FLUENT, the linear interpolations between the points are used. The hydrogen molar fraction in the dome approximately corresponds to that in the top of the acceleration tube.

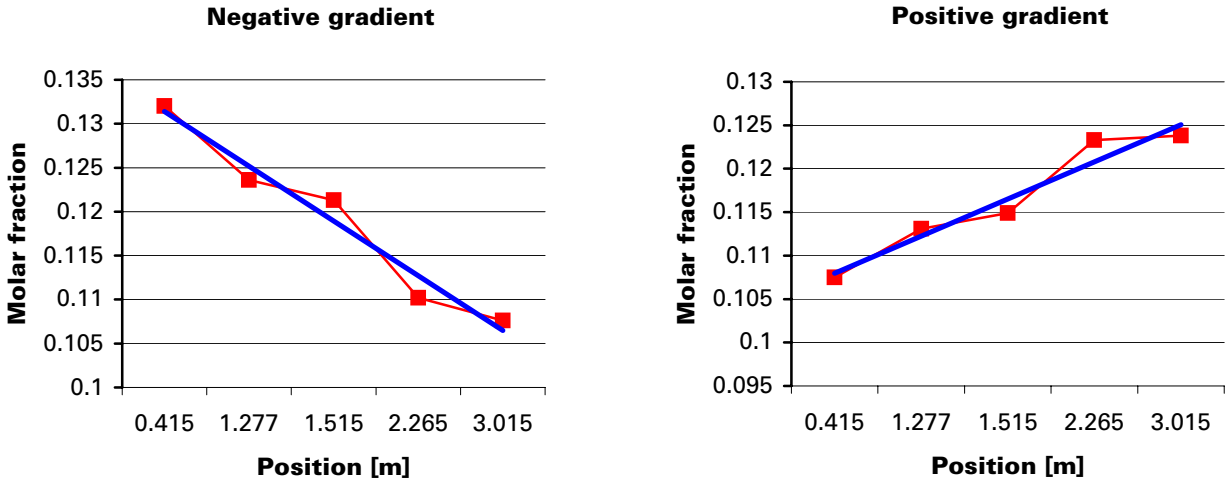

Figure 3. Hydrogen molar fractions along the vertical position of the acceleration tube in case of (a) negative gradient (b) positive gradient.

5 Simulation models

5.1 TONUS combustion models

5.1.1 CREBCOM model

The CREBCOM combustion model is the principal tool for combustion analysis in TONUS. The model has been developed for the simulation of combustion in geometries which are larger than the characteristic dimensions of the physical phenomena involved [1, 2, 7]. The thermal conduction and species diffusion, which are the dominating phenomena in deflagration propagation, are not directly modeled: their action is taken into account by introducing an experimentally derived correlation source term into the Euler equations. The governing equations of the model are

$$\frac{\partial \rho}{\partial t} + \vec{\nabla}\cdot(\rho\vec{u}) = 0 \tag{1}$$

$$\frac{\partial \rho Y_k}{\partial t} + \vec{\nabla}\cdot(\rho\vec{u}Y_k) = \rho\dot{\omega}_k \tag{2}$$

$$\frac{\partial \rho\vec{u}}{\partial t} + \vec{\nabla}\cdot(\rho\vec{u}\otimes\vec{u} + P\mathrm{I}) = \rho\vec{g} \tag{3}$$

$$\frac{\partial \rho e_{tot}}{\partial t} + \vec{\nabla}\cdot(\rho\vec{u}h_{tot}) = \rho\vec{g}\cdot\vec{u} - \rho\sum_k \Delta h_{f,k}\dot{\omega}_k + S_{cr} \tag{4}$$

$$\frac{\partial K_0}{\partial t} + \vec{\nabla}\cdot(\rho\vec{u}K_0) = 0 \tag{5}$$

$$\frac{\partial Y_{H2,f}}{\partial t} + \vec{\nabla}\cdot(\rho\vec{u}Y_{H2,f}) = 0 \tag{6}$$

$$\frac{\partial Y_{H2,i}}{\partial t} + \vec{\nabla}\cdot(\rho\vec{u}Y_{H2,i}) = 0 \tag{7}$$

The combustion progress variable is defined as

$$\xi(\vec{r},t) = \frac{Y_{H2}(\vec{r},t) - Y_{H2,i}(\vec{r},t)}{Y_{H2,f}(\vec{r},t) - Y_{H2,i}(\vec{r},t)} \tag{8}$$

and the reaction rate for the progress variable

$$\dot{\omega}_\xi = \frac{K_0}{\Delta x}\cdot\{\text{criterion\_function}\} \tag{9}$$

where K_0 is a model parameter and Δx the mesh dimension. For a 3D computational cell i the criterion function is equal to 1.0 if the following condition is valid

$$\varepsilon^2 < \sum_{j\in\{\text{neighbours of i}\}} \left(\xi_j^2 - 0.5\xi_i^2\right) \tag{10}$$

where j denotes the set of cells which have a common interface with cell i. In case the condition is not valid, the criterion function is equal to 0.0 and no combustion occurs in the cell. Here, the value 0.5 is used for ε.

The model key parameter is K_0 which defines the combustion rate. It can be determined by trial-and-error or by experimental correlations. The following three methods are available for deflagration regime. Method I is described by Efimenko in [7]:

$$K_0 = S_T\frac{\sigma+1}{4} = \frac{S_T}{S_L}\frac{\sigma+1}{4}S_L \tag{11}$$

The turbulent burning rate S_T is found by experimental correlations

$$\frac{S_T}{S_L} = 0.5(\sigma-1)\frac{L}{\delta}^{1/3} Le^{-2/3}\ \text{, high turbulence L/}\delta\text{>500}$$
$$\frac{S_T}{S_L} = 0.0008(\sigma-1)^3\frac{L}{\delta}\ \text{, low turbulence L/}\delta\text{ < 500} \tag{12}$$

where S_L is the laminar burning rate, L the integral length scale of turbulence, δ the laminar flame thickness and σ the expansion ratio. Method II is described by Dorofeev [6]:

$$K_0 = S_T\frac{\sigma+3}{8} = \frac{S_T}{S_L}\frac{\sigma+3}{8}S_L \tag{13}$$

Method III is described in [11]:

$$K_0 = 66.7\cdot S_L \tag{14}$$

A finite volume approach is used in the discretisa-

tion of the equations. The convective fluxes are discretised by the Van-Leer-Hänel Flux Vector Splitting Method or by the Colella-Glas Scheme (Shock-Shock Method).

5.1.2 *k-ε* and Eddy Break-Up models

In TONUS, alternatively to the CREBCOM model combustion and fluid flow can be modelled by the Reynolds-Averaged Navier-Stokes equations with *k-ε* closure model in which the chemical reaction is modelled by an Eddy Break-Up (EBU) model. A detailed description of the model is given i.e. in Beccantini & Kudriakov [2] but we shall briefly repeat the modelling principles here. The governing equations of the model are

$$\frac{\partial \rho}{\partial t} + \vec{\nabla}\cdot(\rho\vec{u}) = 0 \tag{15}$$

$$\frac{\partial \rho\vec{u}}{\partial t} + \vec{\nabla}\cdot(\rho\vec{u}\otimes\vec{u} + P\mathrm{I}) = \vec{\nabla}\tau^{t} + \rho\vec{g} \tag{16}$$

$$\frac{\partial \rho e_{tot}}{\partial t} + \vec{\nabla}\cdot(\rho\vec{u}h_{tot}) = \vec{\nabla}(\tau^{t}\cdot\vec{u} - \vec{q}) + \rho\vec{g}\cdot\vec{u} - \dot{\omega}_{T} \tag{17}$$

$$\frac{\partial \rho Y_k}{\partial t} + \vec{\nabla}\cdot(\rho\vec{u}Y_k) = \vec{\nabla}\left\{(\rho D_k + \frac{\mu_t}{Sc_{kt}})\vec{\nabla}(Y_k)\right\} + \dot{\omega}_k \tag{18}$$

$$\frac{\partial \rho k}{\partial t} + \vec{\nabla}\cdot(\rho\vec{u}k_k) = \vec{\nabla}\left\{(\mu + \frac{\mu_t}{\sigma_k})\vec{\nabla}(k)\right\} + P_k + G - \rho\varepsilon \tag{19}$$

$$\frac{\partial \rho\varepsilon}{\partial t} + \vec{\nabla}\cdot(\rho\vec{u}\varepsilon) = \vec{\nabla}\left\{(\mu + \frac{\mu_t}{\sigma_\varepsilon})\vec{\nabla}(\varepsilon)\right\} + C_{\varepsilon 1}\frac{\varepsilon}{k}P_k + C_{\varepsilon 1}(1 - C_{\varepsilon 3})\frac{\varepsilon}{k}G - C_{\varepsilon 2}\rho\frac{\varepsilon^2}{k} \tag{20}$$

Eq. (19) represents the turbulence kinetic energy and Eq. (20) the turbulence dissipation rate. In these equations the production term and the gravity term are

$$P_k = \mu_t\left(S_{ij}\frac{\partial u_i}{\partial x_j}\right) - \frac{2}{3}\rho k\vec{\nabla}\cdot\vec{u} \tag{21}$$

(22)

The constants used in this model are:

$\sigma_k = 1$ $\quad \sigma_t = 0.7$ $\quad \sigma_\varepsilon = 1.3$
$C_{\varepsilon 1} = 1.44$ $\quad C_{\varepsilon 2} = 1.92$ $\quad C_{\varepsilon 3} = 1$ if G<0
$C_{\varepsilon 3} = 0$ if G>0

The Eddy Break-Up model for combustion assumes that the reaction rate is limited by turbulent mixing. In the model based on the work of Spalding [12] the reaction rate is given by

$$\dot{\omega} = -C_{EBU}\rho_{H2}\frac{\varepsilon}{k}\left(1 - \frac{Y_{H2}}{Y_{H2,i}}\right) \tag{23}$$

where the index i refers to initial value. In this study C_{EBU} = 5 is used. This value is suggested by Cant [5] for combustion in closed volumes.

The turbulence model in TONUS V.2006 is somewhat limited because it does not include near-wall treatment but wall functions are currently being incorporated into the code.

5.2 FLUENT combustion model

Combustion is modelled with Eddy break-up (or Eddy-dissipation) model, which is based on a modification of Eq. 23 by Magnussen & Hjertager [9]. The naming convention depends on the source. In this approach it is assumed that turbulent mixing rather than chemical kinetics controls combustion. Turbulence mixes the species, hydrogen and oxygen and the rate of the mixing process limits combustion. In this particular case air and hydrogen have been premixed and turbulence is considered to wrinkle the flame front and mix the active radicals to the unburnt combustible mixture. The reaction rate of hydrogen is calculated from Equation (24). The last term including mass fraction of the products restricts ignition in domains where the flame front has not yet proceeded.

$$R_{H_2} = A\rho\frac{\varepsilon}{k}\min\left(m_{H_2}; \frac{m_{O_2}}{s_{O_2}}; B\frac{m_{prod}}{s_{prod}}\right) \tag{24}$$

The term ε/k describes the rate of turbulent mixing. The constants A and B are 4.0 and 0.5 respectively. k and ε are kinetic energy and dissipation of turbulence and ρ density of mixture. m_{H_2}, m_{O_2} and m_{prod} are the mass fractions of hydrogen, oxygen and products. si is the stoichiometric ratio of relevant species.

Turbulence is calculated by using the two-equation *k-ε* model which is described in the previous section. On the walls the standard wall functions of the code are applied. When wall functions are used, the allowed maximum distance to the first cell centre depends on flow velocity by the wall. In the present case, when flow velocity varies in large

range, the wall cell is generally small enough but may exceed the optimal size at the extreme velocity values.

5.3 Simulation set-up

5.3.1 Grids used in TONUS

Several 2D and 3D grids have been tested using the CREBCOM and EBU models. The basic grid used for CREBCOM 2D calculation (positive gradient case) is shown in Figure 4a. A more fine 2D mesh, shown in Figure 5a, was used for the k-ε computations. The average dimension of this grid corresponds to the full 3D mesh used in FLUENT calculation described in the next section, i.e. the square root of a computational cell area is approximately the cubic root of a cell volume in the 3D case. The 3D grid used in TONUS for CREBCOM calculations represent a quarter of the geometry as shown in Figure 6 and Figure 7. In the grid figures, the red

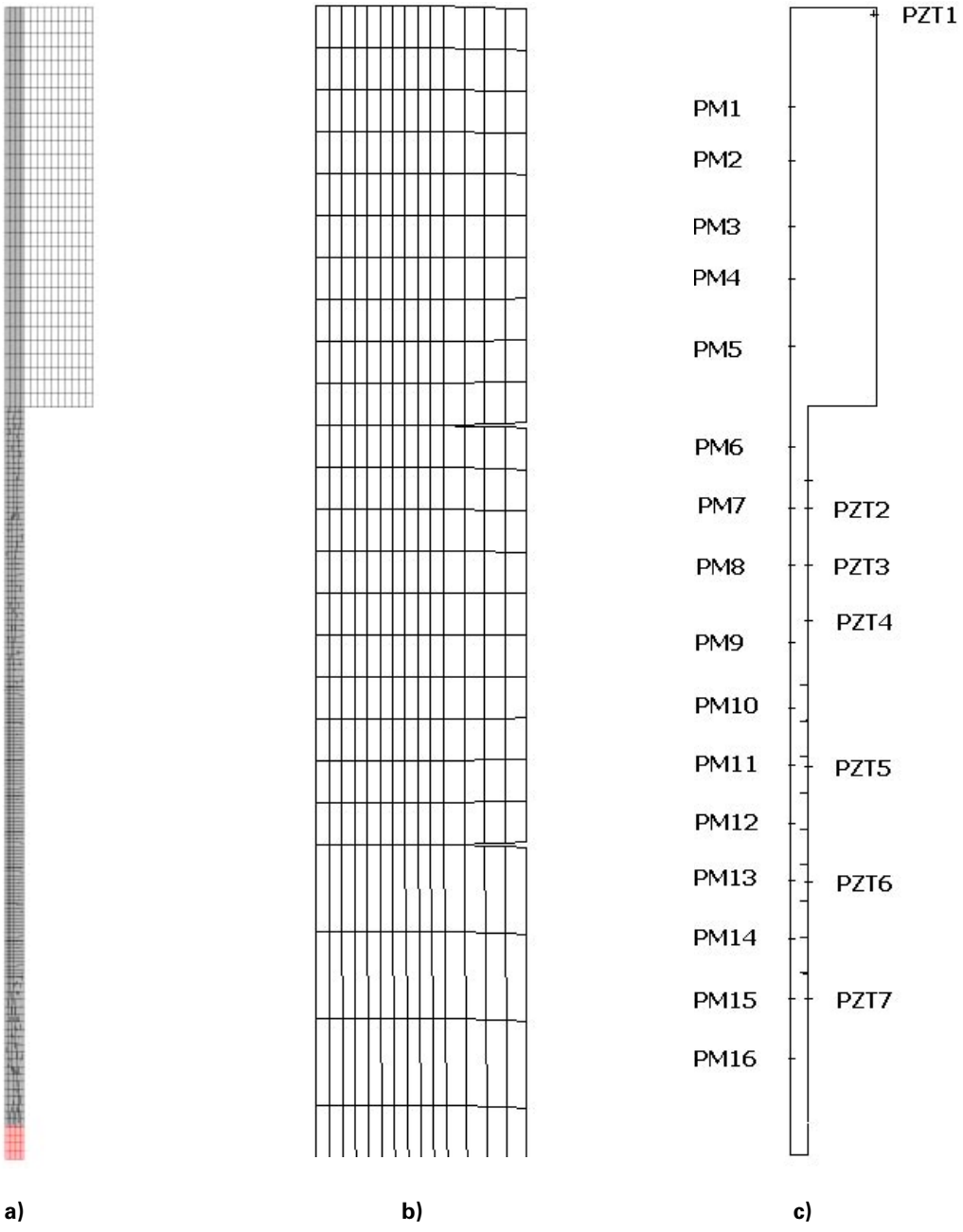

Figure 4. (a) Basic 2D grid used in TONUS simulations using CREBCOM model. **(b)** A detail of the grid in the beginning of the obstacle section. **(c)** The transducer positions in the grid.

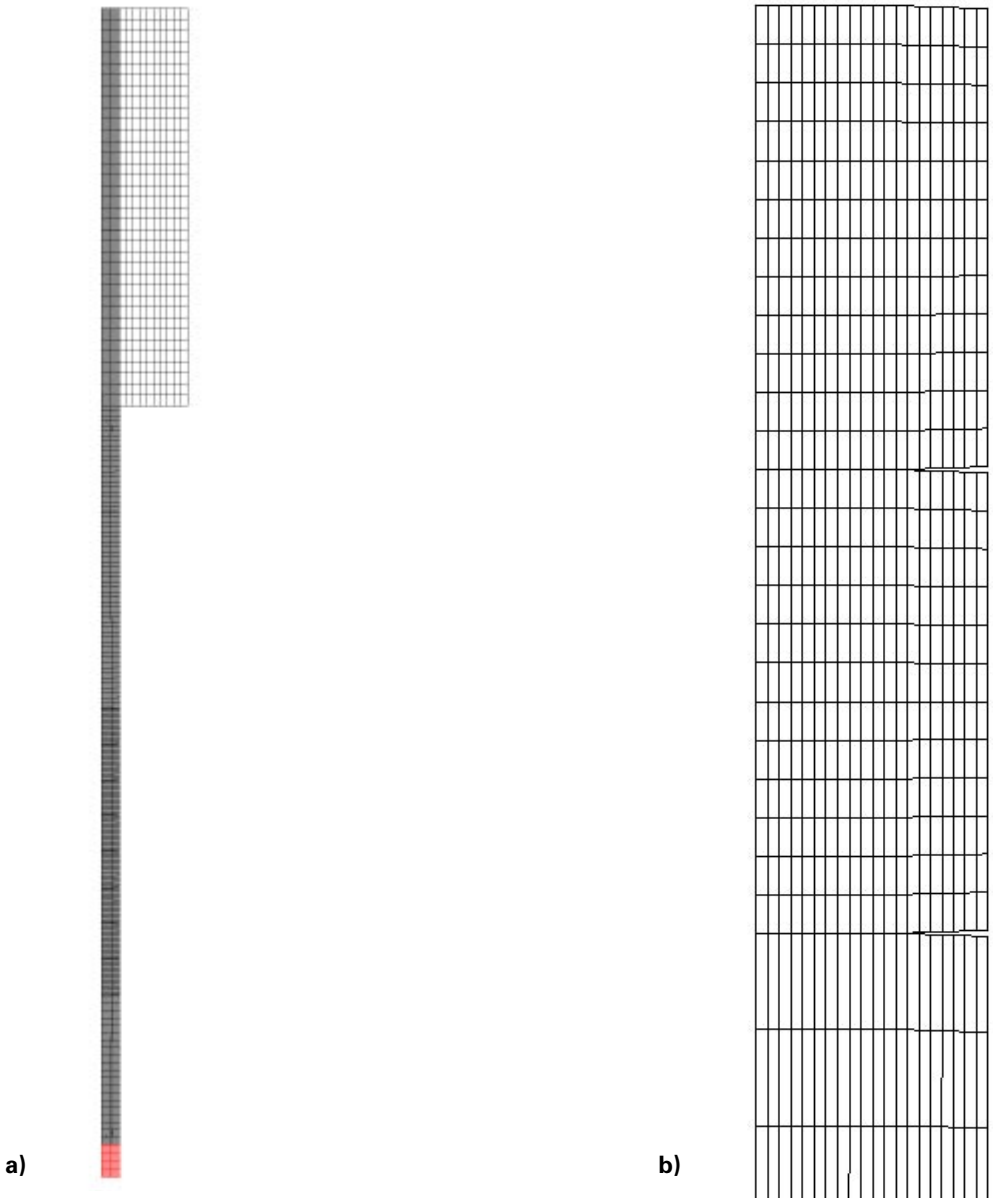

Figure 5. (a) The fine 2D grid used in TONUS for *k*-*ε* and EBU model simulations. **(b)** A detail of the grid in the beginning of the obstacle section.

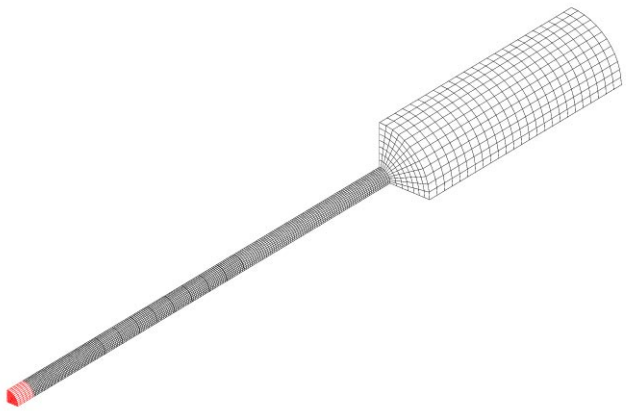

Figure 6. 3D grid used in TONUS simulations using CREBCOM model.

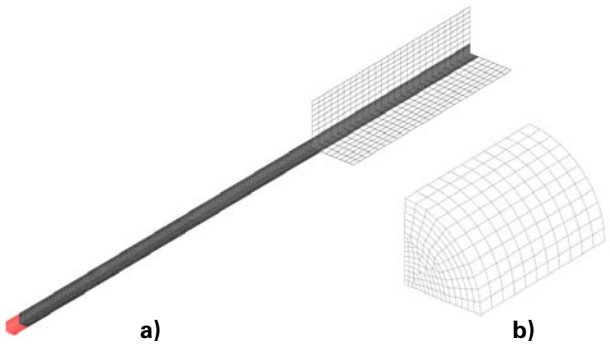

Figure 7. (a) A view of the symmetry planes of the 3D grid. **(b)** A part of the obstacle section in the acceleration tube.

Table 2. Computational grid information.

Grid	Number of elements	Average element area/volume	Δx
2D basic	2 876	3.0370^{-4} m²	0.0175 m
2D fine	4 680	1.8828^{-4} m²	0.0137 m
3D	32 005	$6.1419 \cdot 10^{-6}$ m³	0.0183 m

area seen in the bottom of the grid is the zone which is used to simulate ignition. The characteristics of each grid are given in Table 2.

The annular obstacles are modelled by "cracks" with a triangular cross-section in the domain as shown in Figure 4b and Figure 5b. The width of the obstacle at its base at the wall is 2mm. The locations of the pressure transducers (PZT) and photomultipliers (PM) are shown in Figure 4c. The pressures are captured near the walls.

5.3.2 Grid used in FLUENT

The FLUENT calculation is performed using one full 3D grid without symmetry planes. The number of computational cells is 195 312. The cross section of the grid is shown in Figure 8.

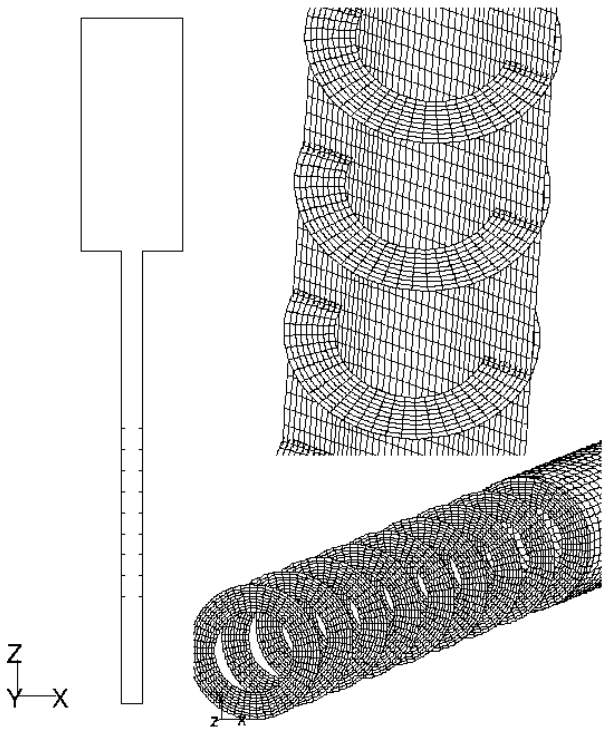

Figure 8. Cross sections of the computational grid. Length of the tube is 3 m and height of the dome 2 m.

5.3.2 Initial and boundary conditions

In the present TONUS CREBCOM simulations the parameter K_0 which is the key parameter in calculating the combustion rate is taken as constant. For the uniform mixture K_0 = 10.5 m/s and for the negative concentration K_0 = 8.0 m/s are used. These values are calculated for average hydrogen concentrations of 13% and 12.3% by Bentaib al. [4]. For the positive gradient case K_0 is defined by trial-and-error by investigating the effect of changing the value.

The ignition in TONUS is modelled by assuming that the gas in the bottom of the channel is already burnt by defining in the cells below the point of ignition the theoretical AIBC final conditions. Then the combustion starts to advance upward. If the CREBCOM model is used, it is necessary that the ignition zone is large enough, i.e. to give the burnt gas conditions in several adjacent cells. Otherwise, the criterion function (Eq. 10) may have a zero value and the mixture is not ignited.

In both FLUENT and TONUS Eddy Break-up model simulations the ignition and the laminar combustion phase are not modelled in detail. In reality, turbulence has not been developed yet after the initial ignition. In this phase the flame front proceeds according to the laminar flame velocity. In the simulations the ignition phase is described by introducing an initial turbulence to the ignition location. As a consequence, the initial flame velocity varies with the initial turbulence. Later when the flow field generates its own much stronger turbulence, the initial definitions are not important.

In FLUENT the ignition zone consists of 49 cells surrounding the point of ignition with volume of 2.6·10–5m³, which is small compared to the total modelled volume 0.7862 m³. To this ignition zone a small amount of steam and higher values of temperature and turbulence parameters have been imposed. The initial values used for turbulence parameters k and ε in the ignition zone in the homogenous mixture and negative mixture gradi-

ent FLUENT calculations are k= 10 m²/s² and ε = 10000 m²/s³. In the positive mixture gradient case the values are the same with the exception of ε = 1000 m²/s³. For the rest of the flow field the initial values are

k= 0.01 m²/s²

ε = 0.01 m²/s³

In the TONUS Eddy Break-up calculations the ignition zone and AIBC condition similar to the CREBCOM cases are used with the addition of imposing initial turbulence values k= 0.1 m²/s² and ε = 0.1 m²/s³ to the flow field.

Second order time discretisation and explicit solver were used in TONUS calculations. In FLUENT calculations, the time dependent transient was run using 0.1 ms time step. The space and time discretisation were second order accurate.

In FLUENT simulations, the system walls are represented by the standard no-slip wall boundary condition of the code. In the TONUS k-ε simulation a frictionless wall is used due to lack of near-wall treatment in the model. No heat losses to the environment are taken into account in TONUS or FLUENT simulations. The effect of heat losses on the results in previous TONUS simulations of the ENACCEF tests has been studied by Malet [10] who observed it to be very small.

6 Simulation results

6.1 TONUS

6.1.1 CREBCOM model calculations

Figures 9–11 represent the pressure histories measured at the transducers PZT1–PZT7 in the three different hydrogen concentration cases in which the 3D grid has been used. The pressure curves consist of the initial pressure wave travelling ahead of the deflagration front which is seen as the first peak in the curves and the following oscillatory pressure build-up to the level of the AICC pressure while all the hydrogen is being consumed. The peak pressure of the deflagration ranges from 484 kPa of the uniform case to the 356 kPa of the positive case.

In Figure 12 the flame position along the facility axis (time of arrival) is given for the three different hydrogen concentration tests. The time of arrival is computed on the basis of the decrease of the hydrogen mass fraction captured at the PM transducer locations at the tube axis. The hydrogen mass fraction has a steep gradient across the reaction zone and the position of the flame front is defined as the axial position in which the mass fraction at the transducer in question has decreased to approximately half of its initial value.

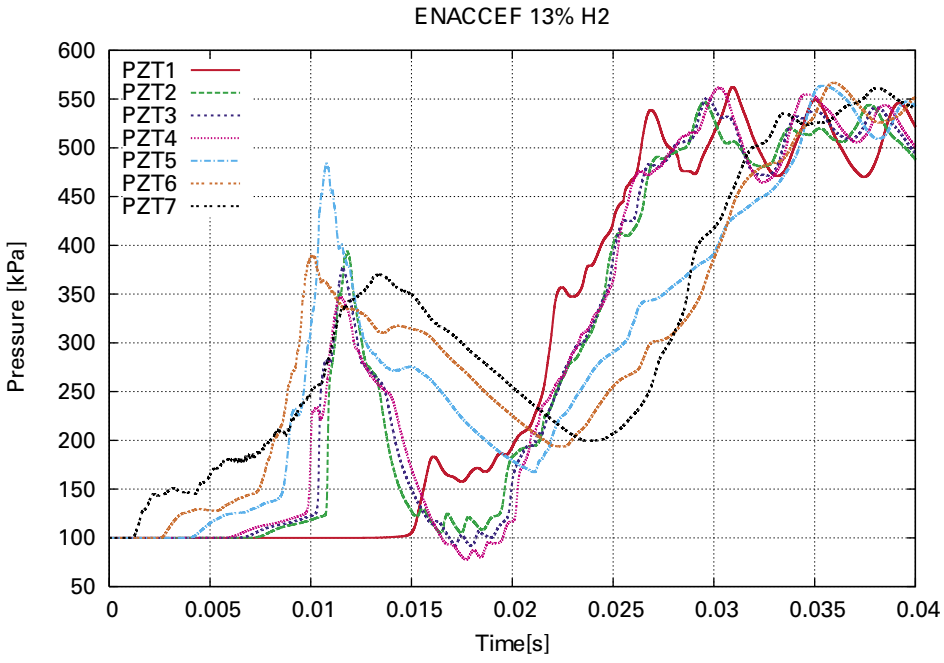

Figure 9. Pressure evolutions at the PZT transducers in 13% H_2 uniform mixture case.

Figure 13 shows the flame speed comparison along the facility axis in the three different hydrogen concentration cases. The end of the acceleration tube and the entrance to the dome is located at about 3.3 m. The profile of the flame speed evolution is similar in all three cases: initially there is

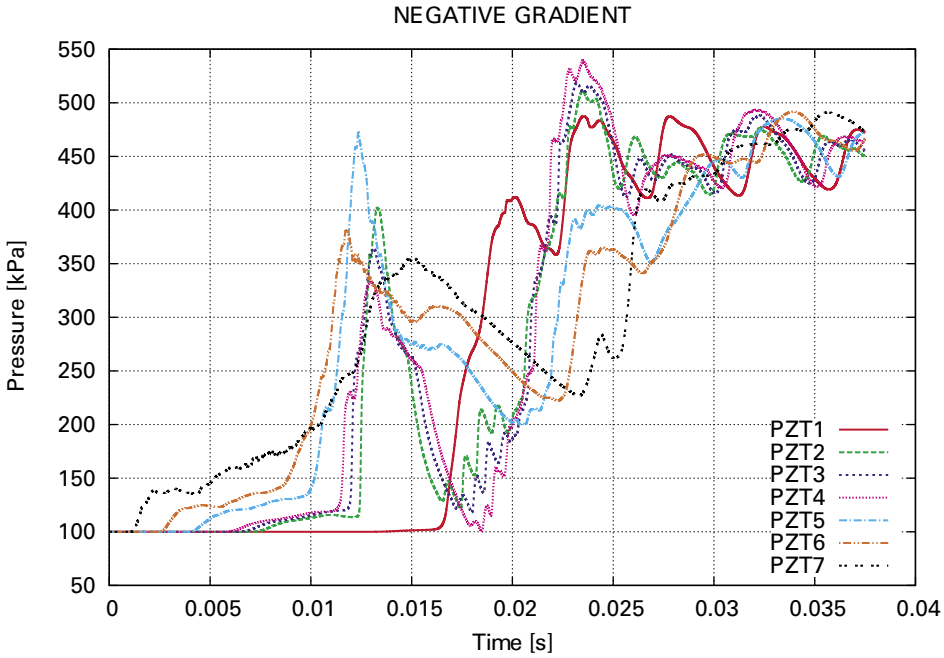

Figure 10. Pressure evolutions at the PZT transducers in the negative H_2 gradient case.

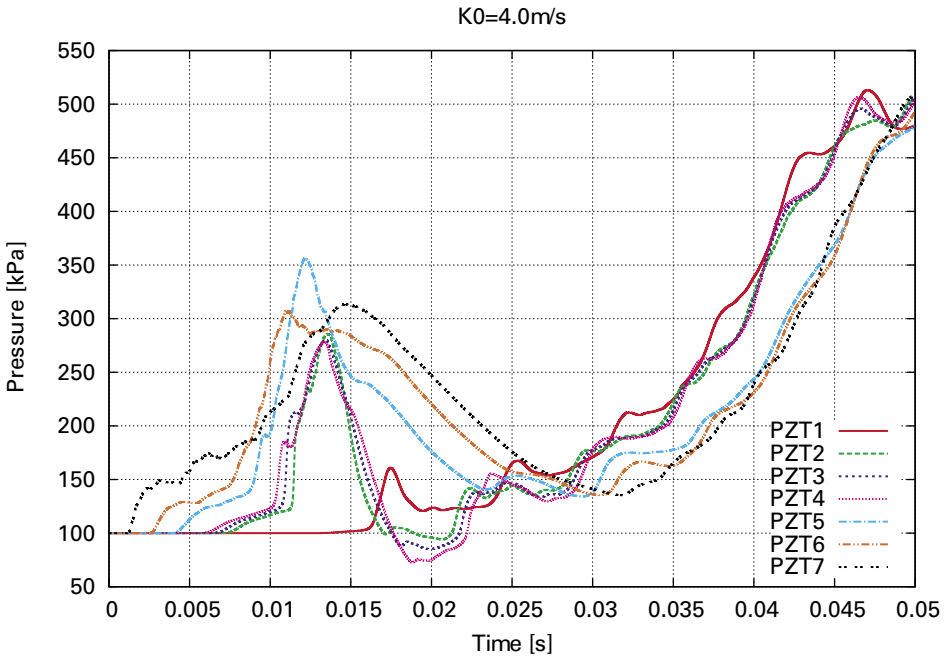

Figure 11. Pressure evolutions at the PZT transducers in the positive H_2 gradient case.

acceleration in the obstacle section, deceleration in the upper part of the acceleration tube with no obstacles and acceleration when the reaction zone enters the dome. Because of the nature of the combustion model, the flame velocities and pressures are smaller in the cases where K_0 is smaller.

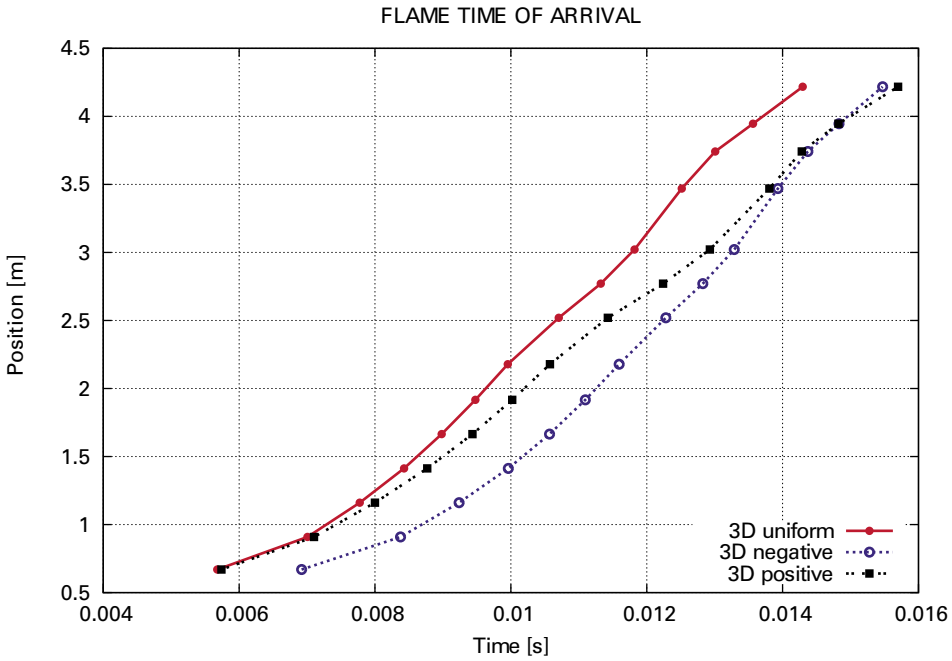

Figure 12. Flame time of arrivals in uniform, negative and positive gradient cases.

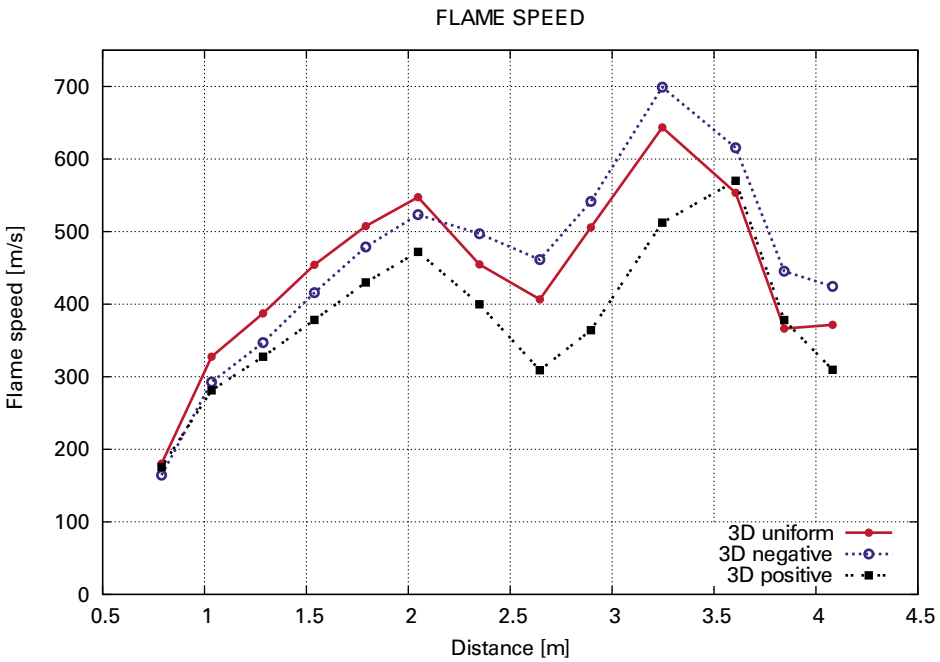

Figure 13. Flame speeds as a function of distance from the bottom in uniform, negative and positive gradient cases.

The contours of hydrogen mass fraction at selected simulation times are shown in Figure 14. It is seen that in the acceleration tube the shape of the flame front is very sharp as the obstacles restrict the flow near the walls. There are "pockets" of unburnt gas at the wall between the obstacles after the flame has advanced to the upper part of the tube. After reaching the dome the flame front advances quickly to the top of the dome in the middle of the channel but the horizontal combustion towards the walls of the dome is significantly slower. It is likely that this is a numerical effect. The grid in the middle of the channel is much finer compared to the rest of the dome which results in reduced numerical diffusion toward the side walls. In addition, the reaction rate in the CREBCOM model depends on the cell size. Thus, there is a strong coupling between the flame speed and the grid density in the model.

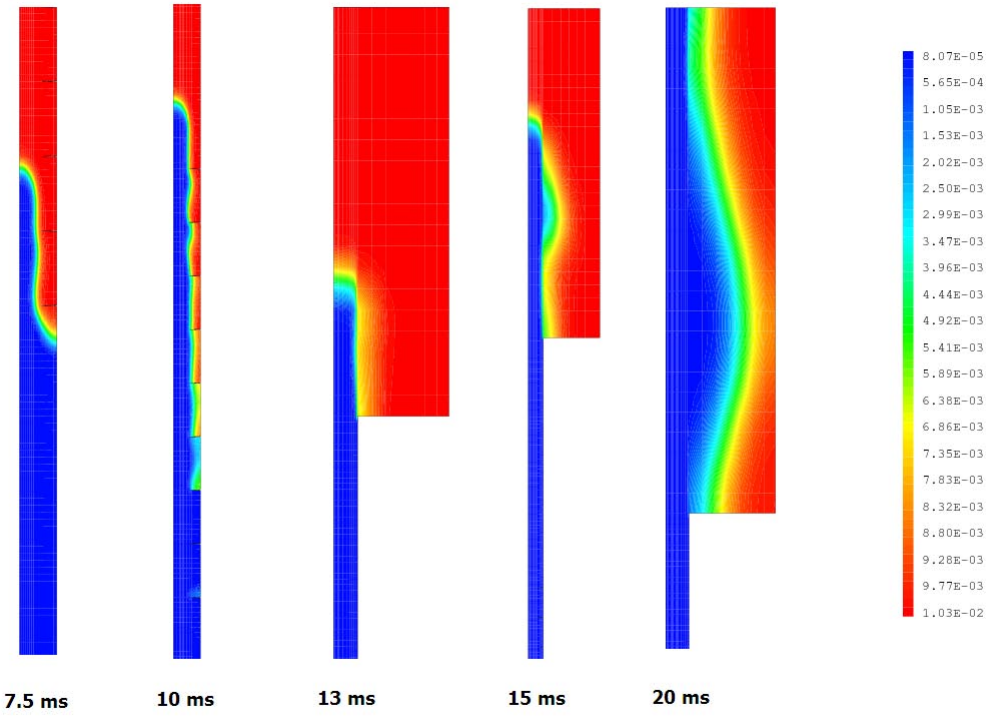

Figure 14. Hydrogen mass fraction at selected simulation times.

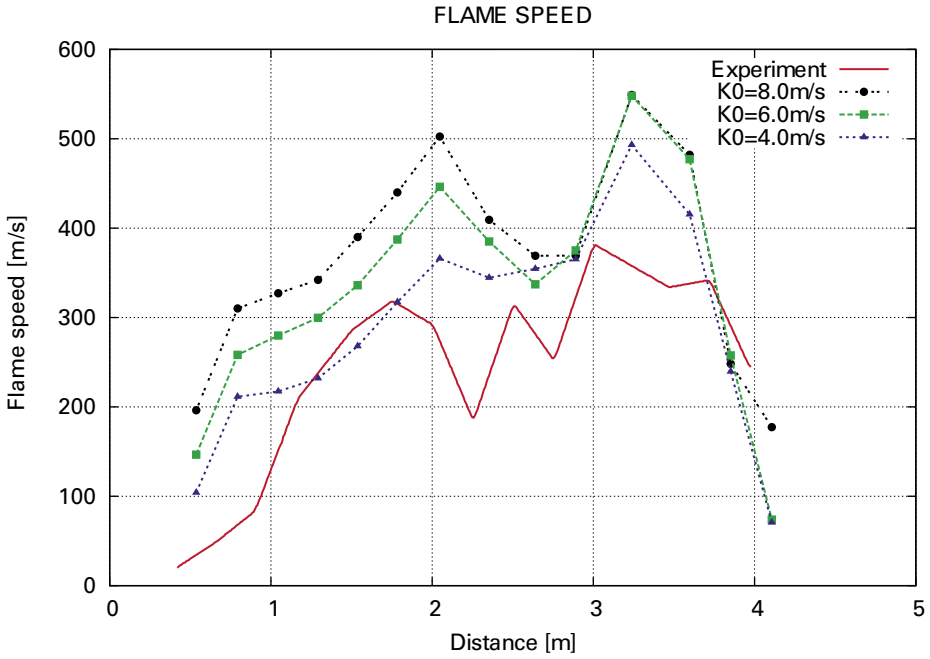

Figure 15. Effect of K_0 on the flame speeds in positive gradient case.

The positive concentration test and the basic 2D grid were used to study the sensitivity of the system behaviour to K_0. The flame speed comparison with K_0 = 4 m/s, K_0 = 6 m/s and K_0 = 8 m/s is shown in Figure 15 in which also a test result reported by Bentaïb [3] has been included. The value 8 m/s was also used in simulations by Bentaïb et al. [4] who calculated the value using Eq. 11 for a hydrogen volume fraction of 12.3%. The average hydrogen volume fraction in the simulated system including the dome is 12.32%. In this 2D case the pre-calculated K_0 results in clearly too high flame velocities. The best estimation is given by K_0 = 4 m/s.

Figure 16 shows the pressure evolution comparison at PZT5 with different K_0. It is observed that the first pressure increase set forth by the deflagration is more drastic if K_0 is increased.

6.1.2 Eddy Break-up model calculations

Figure 17 represents the pressure histories captured at the locations of the transducers PZT1-PZ7. The maximum pressure of the initial compression

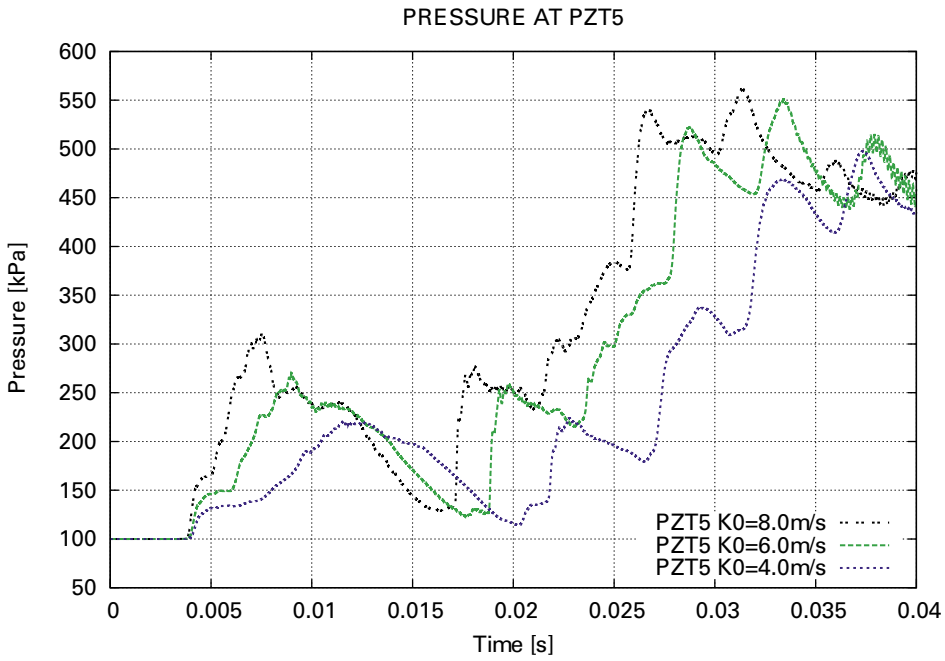

Figure 16. Effect of K_0 on the pressure in positive gradient case.

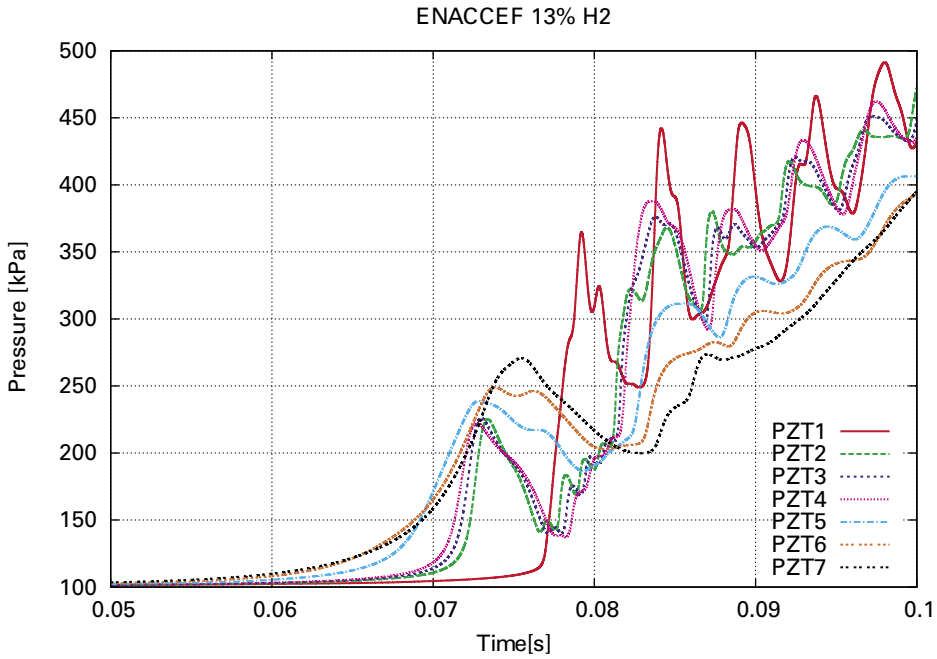

Figure 17. Pressure evolutions at the PZT transducers in 13% H_2 uniform mixture case.

wave varies between 250–270 kPa depending on the measurement location. The magnitude of these pressure peaks is not as high as the final pressure into which the system stabilizes when no heat losses are accounted for. Also, the pressure rise in the first two transducers (PZT7 and PZT6) is not as steep as in the following transducers. Instead, the curves show a gradual rise and decrease rather than a sharp pressure wave. Presumably, this is because of the inaccurate modeling of the ignition in which only the initial arbitrary turbulence affects the flame propagation and the reaction rate is at first very small causing the pressure to rise slowly. The low pressure peaks might be unphysical due to the limitations of the 2D model used in the case (see Chapter 7) or the initial turbulence in the ignition zone and the acceleration tube.

The time of arrival of the flame at the axis of the test tube is shown in Figure 18. There is a sharp jump at 0.07 s when the flame enters the obstacle

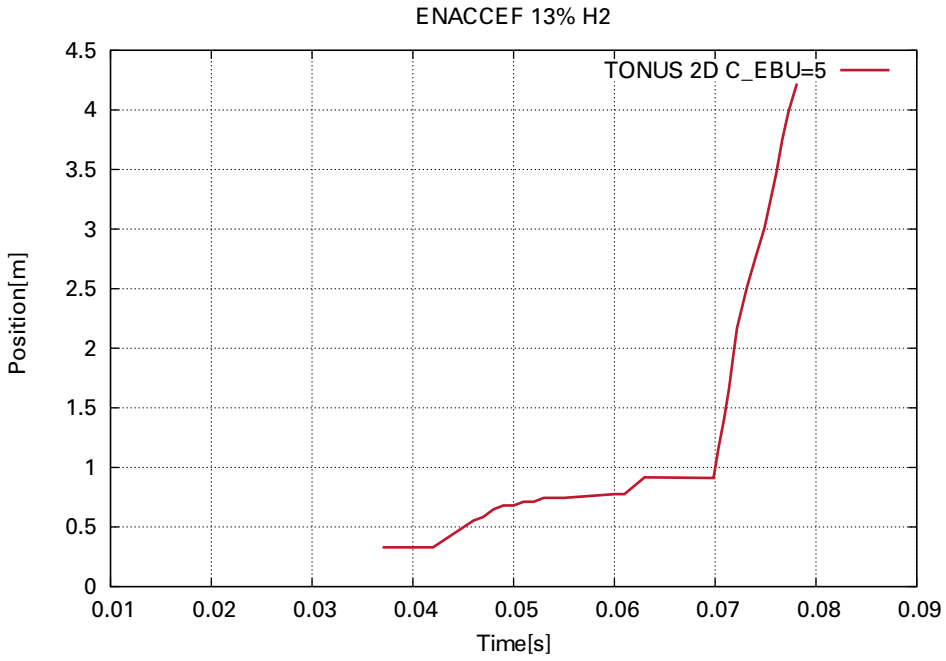

Figure 18. Flame time of arrival.

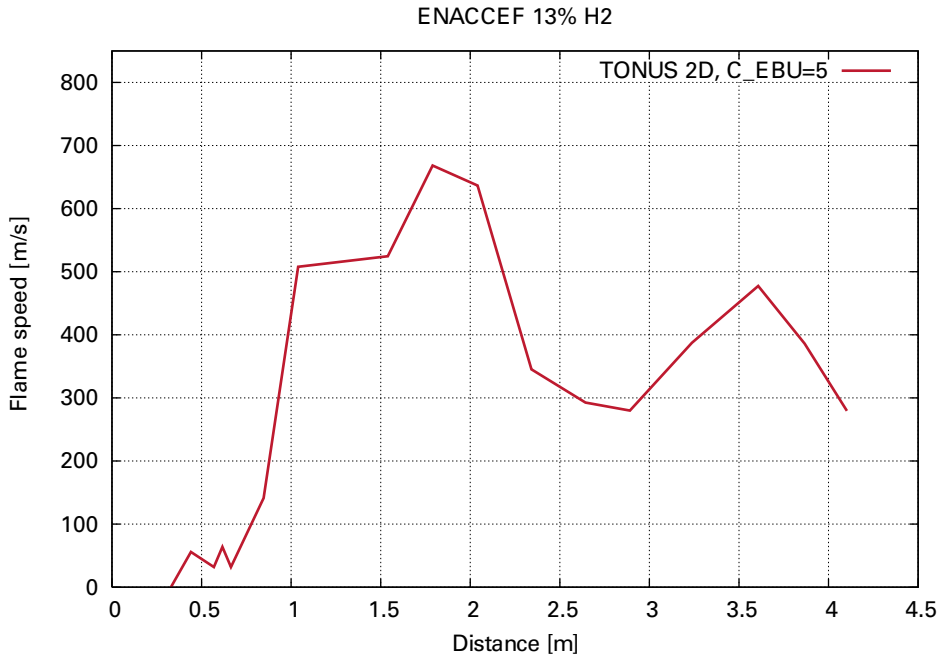

Figure 19. Flame speed as a function of distance from the bottom.

section of the acceleration tube and the enhanced turbulence quickly accelerates the flame. The flame has reached the PM1 transducer in the upper section of the dome at approximately 0.078 s. At this point unburnt gas remains near the top and upper "corners" of the facility cross-section. All the fuel is burnt after 0.1 s.

Figure 19 represents the flame velocity as a function of distance from the bottom of the facility.

Figure 20 shows the mass fraction of hydrogen at selected simulation times. In this case, turbulent mixing spreads the reaction zone into the spaces between obstacles and the flame front is not sharply defined as in the CREBCOM case. In the dome the combustion progress is at first fastest in the corner of the dome bottom and the acceleration tube, and the flame at the axis is following slightly behind. Finally, the flame front proceeds spherically towards the top and side walls of the dome.

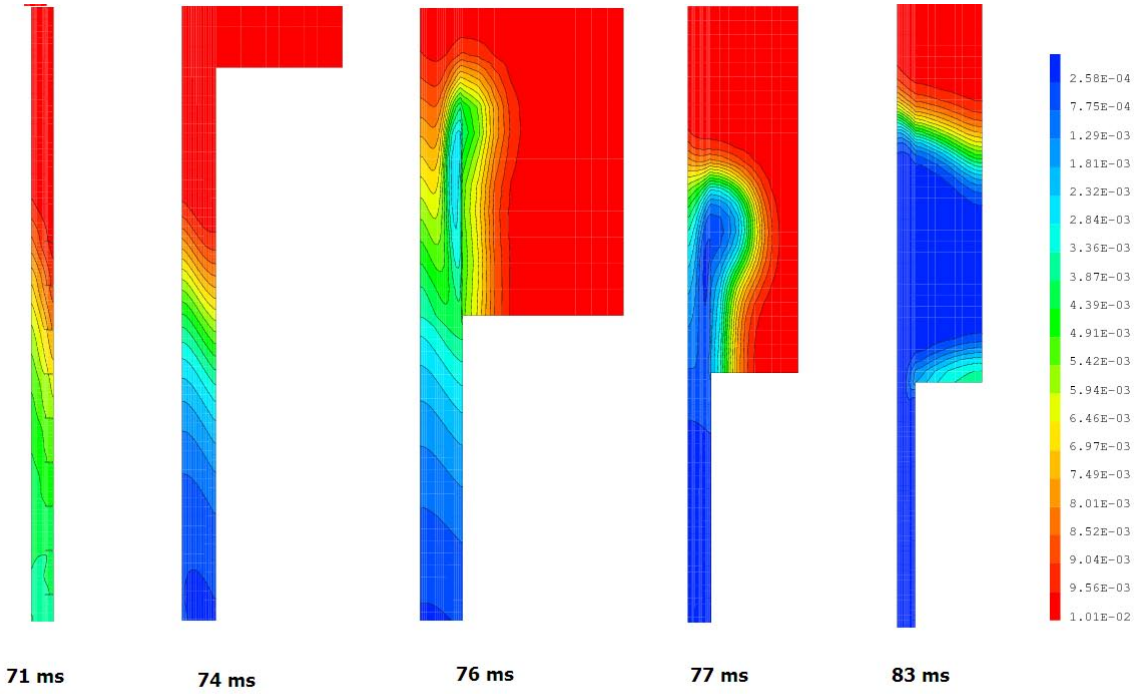

Figure 20. Hydrogen mass fraction at selected simulation times.

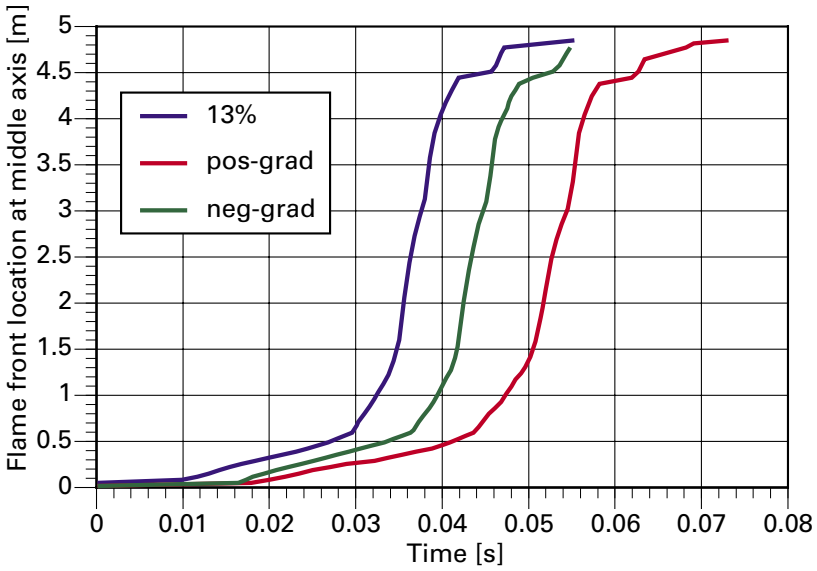

Figure 21. Location of the flame front along the tube axis.

6.2 FLUENT

In the simulation the ignition point, located 0.138 m above bottom, is larger than the spark due to numerical resolution. Flame front proceeds rather slowly first spherically and then along the tube to both directions from the ignition point. Flame front location is traced along the axis of the tube. The front location is shown as a function of time for each case in Figure 21. Up to 30–40 ms the flame front proceeds relatively slowly. At that time the flame has proceeded to the first obstacles. After that combustion is enhanced due to turbulence generated by the ring obstacles. In the obstacle region turbulence has been generated due to flow by expansion already before the flame front has proceeded to that region. Thus acceleration in this region is very quick.

The reaction rate at selected time steps is shown in Figure 22. The enhancement of combustion due to the obstacles is clearly shown. The flame front is corrugated and extended which increases the effective combustion domain. In the obstacle domain the flame first penetrates through the area and after

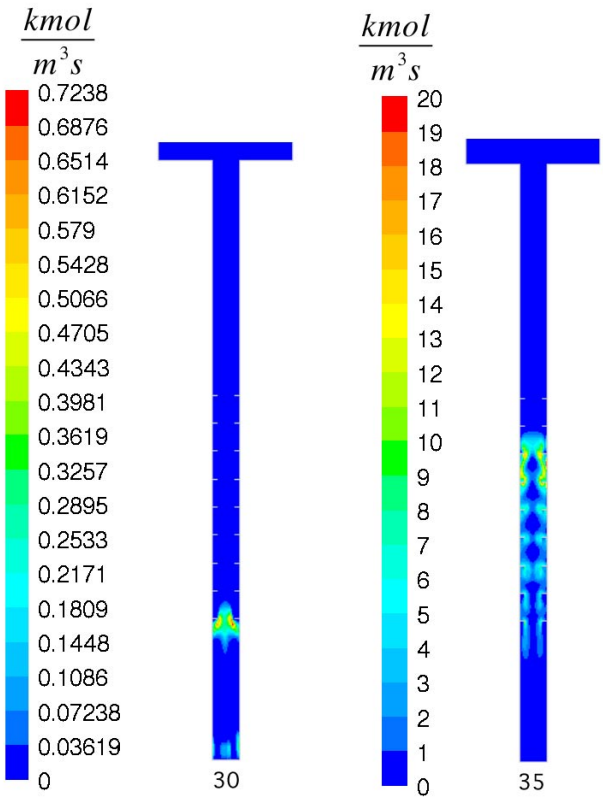

Figure 22. Reaction rate at selected time steps. Time is in ms.

that the flame front proceeds sideways to the tube walls. In the obstacle region the local maximum reaction rates are essentially higher than before or after the obstacles. It is observed that after the obstacle region the flame front proceeds significantly faster close to the tube walls than in the midline. Bulk flow in the tube generates turbulence due to wall friction and affects the time scale of turbulence. A similar feature in the flame front shape is also given in report [8]. In the dome area the flame proceeds much slower (Figure 23). Also due to the pressure fluctuations in the tube the flame front velocity is oscillating, which can be seen from the animation.

Velocity field at selected time steps is shown in Figure 24. After the first expansion the flow field oscillates in the tube, which can be more clearly seen in the animations. The pressure evolutions

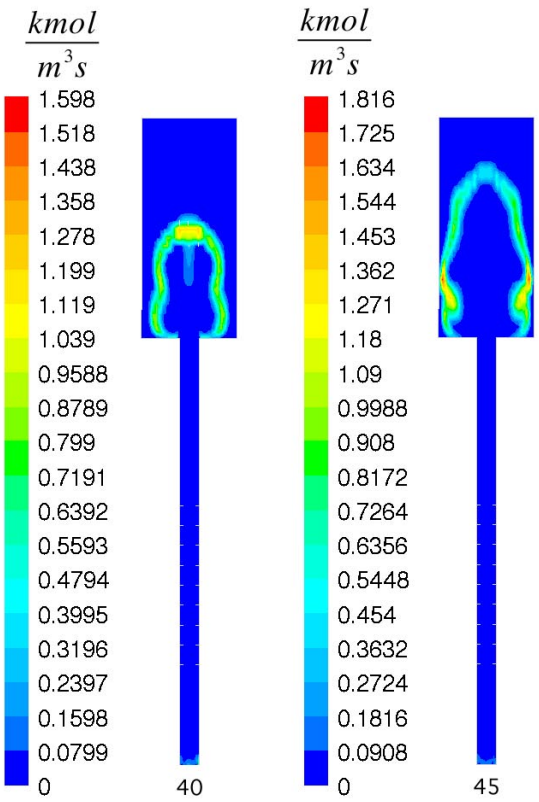

Figure 23. Reaction rate at selected time steps. Time is in ms.

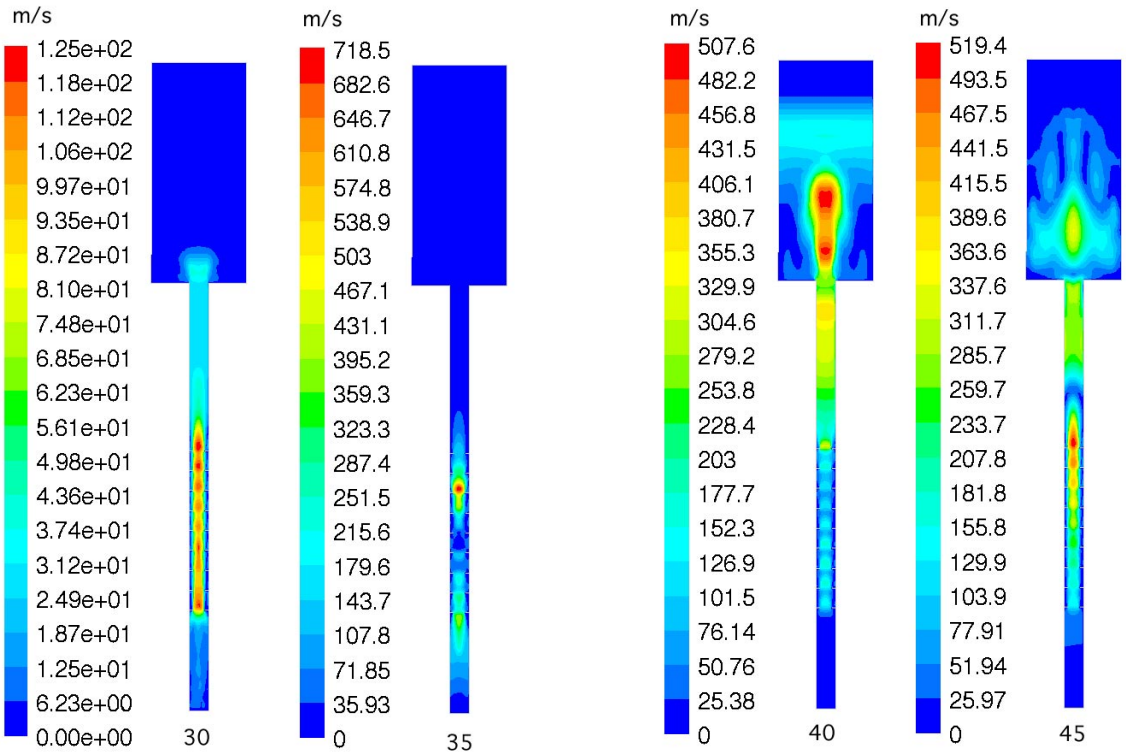

Figure 24. Velocity magnitude at selected time steps: 30 ms, 35 ms, 40 ms and 45 ms.

recorded at the PZT transducer locations are shown in Figure 25. The pressure monitor points PTZ7–5 are located in the obstacle region and PTZ4–2 after the obstacles. The oscillation in the tube is clearly shown.

Figure 26 shows the pressure development in top the vessel and inside the rings at all concentration gradient cases. In the positive gradient case the pressure rise starts later, due to longer ignition time. The end pressure is almost same as in the homogeneous case. In negative gradient case the end pressure is lowest due to the lower hydrogen concentration in the large dome area.

The flame front velocity has been calculated from flame position shown in Figure 21. The result is shown in Figure 27. In this figure the flame is traced along the tube axis. In the tube after the obstacles, flame front propagation near the tube walls is faster than on the axis. This can be seen as a dip near the end of the tube, at 3 m. The transients were computed until 100–120 ms so that average pressure has gained its local value. Pressure oscillations are still present at that stage.

The implementation of flame tracking in FLUENT simulation is not strictly the same as in the instrumentation. In the simulation the flame front is tracked along the axis whereas the optical sensor is able to see through the cross section of the tube. Also the flame front velocity in the dome should be defined better in the simulation.

The average pressure and total reaction rate in negative gradient case is shown in Figure 28. The velocity of flame front is shown as a function of time in Figure 29. The essential front propagation takes

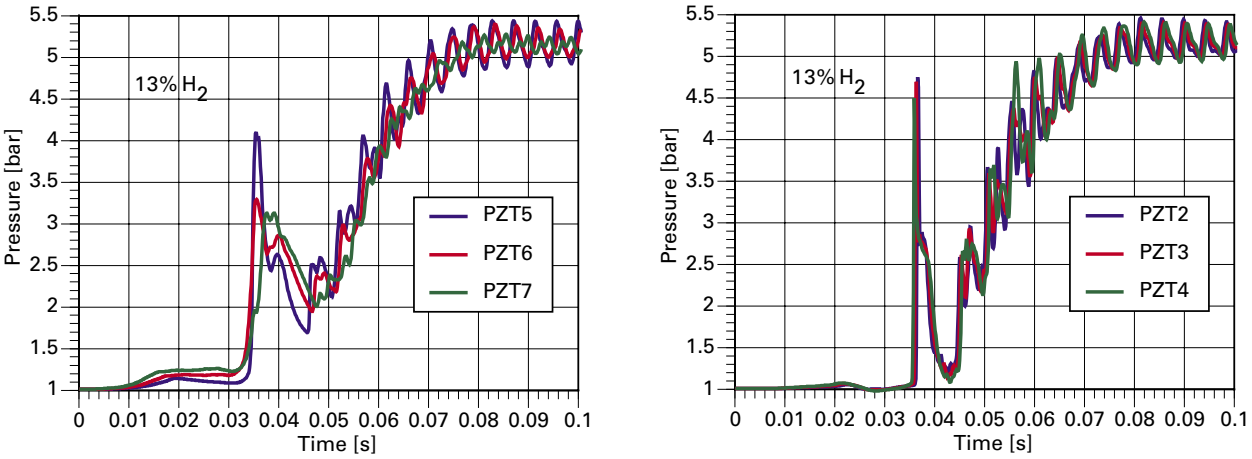

Figure 25. Absolute pressure development in locations nearest to the ignition point. Homogeneous mixture. Point PZT7 is located before the obstacles, PZT6 between rings 3–4, PZT5 between rings 6û7 and PZT4–2 after the obstacles.

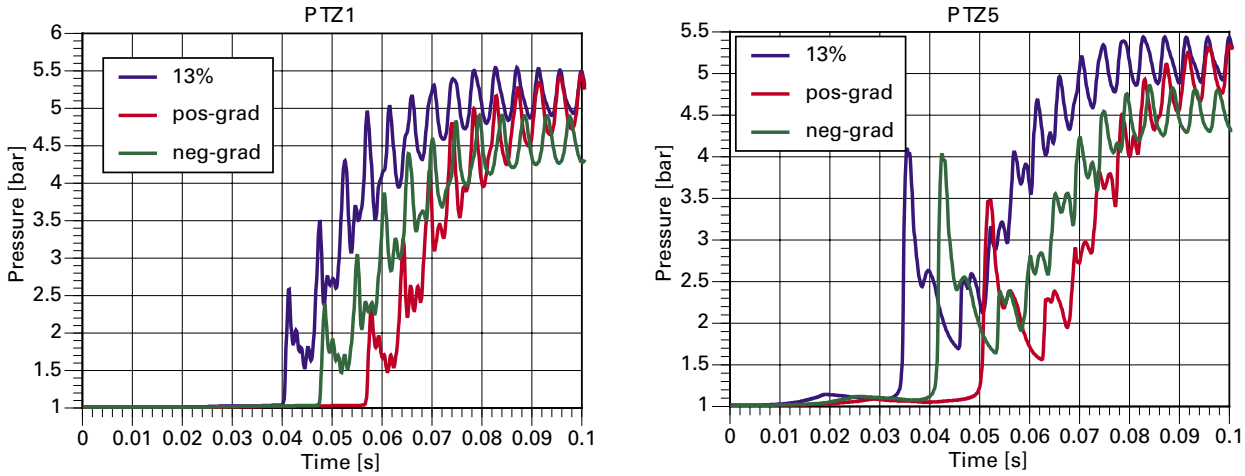

Figure 26. Pressure development in monitor points PTZ1 (top of the dome) and PTZ5 (between rings 6–7).

place in very short time interval. In the simulation the temporal resolution is 0.1 ms. The spatial resolution is one computational cell, which in z-direction is about 0.01–0.04 m in the tube area. At the most violent stage the front may proceed one cell in a time step. Both the temporal and spatial resolution can be refined for better accuracy.

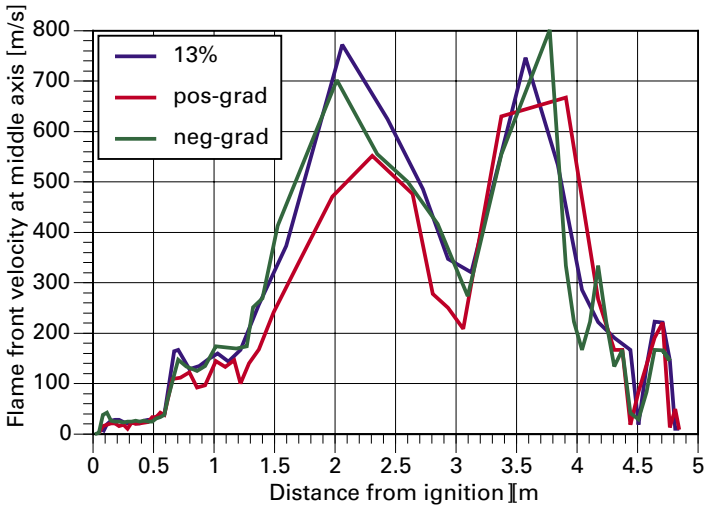

Figure 27. Flame front velocity along the tube axis calculated with Fluent.

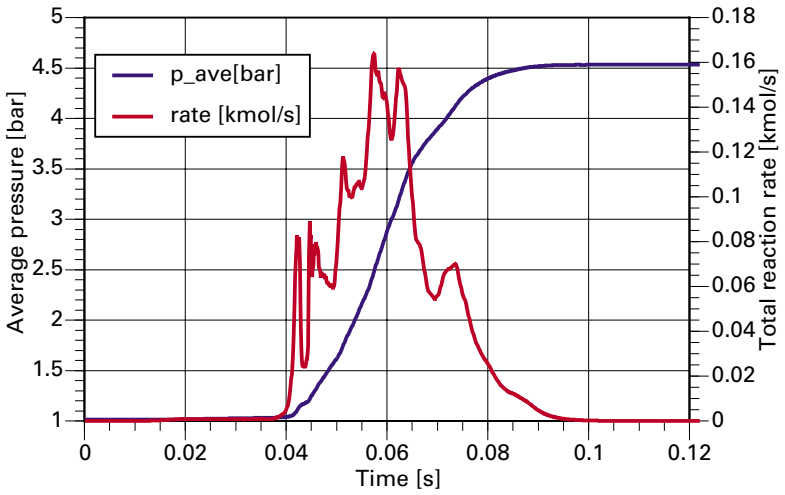

Figure 28. Average pressure and total reaction rate as function of time in negative gradient case.

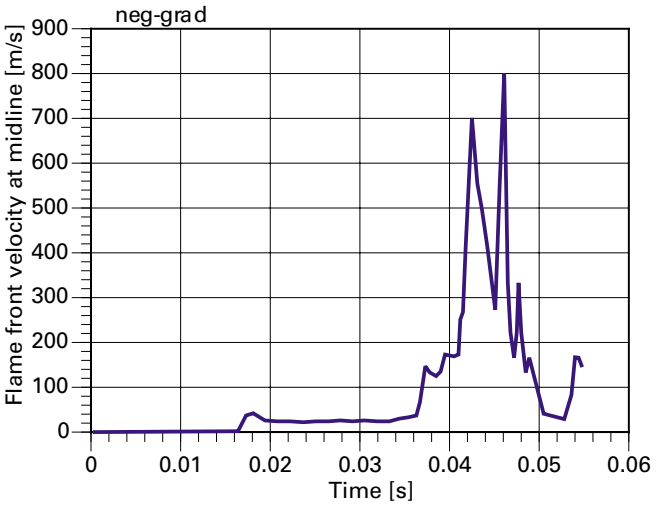

Figure 29. Flame front velocity as a function of time in negative gradient case.

6.3 Comparison of results

In this section the TONUS and FLUENT results are compared to each other and to the experimental flame speed data presented in Bentaib [3]. Figures 30–32 present the flame speed comparisons to the test results.

In the uniform mixture case the flame acceleration and maximum velocity in the acceleration tube shows a relatively good agreement with the test results. Around the entrance to the dome the second acceleration phase is overestimated. Fluent tends to give the highest flame peak velocity. This may partly be a consequence of limited axial resolution as noted in Chapter 6.2. The general behaviour is same in all simulations. All predict the second acceleration in the dome to be stronger that the experimental values suggest.

In the negative gradient case the calculated flame speed profile resembles the one in the homogenous mixture with the exception that the peak velocity is lower in the obstacle section but slightly higher in the dome section. The flame acceleration is also weaker in the obstacle section than the corresponding acceleration in the test result. In the test result, a sharp drop is observed in the upper part of the acceleration tube and the flame front velocity increases only slightly as it enters the dome at 3.3 m. These are the parts of the facility where the initial hydrogen volume fraction was lowest. Interestingly, in addition to the flame speed reported for SARNET benchmark exercise [3] a previous study by Bentaib et al. [4] states that the flame speed profile in a negative concentration is similar to the uniform mixture case. The experimental uniform mixture flame velocity in Figure 30 is identical to that reported in the previous study [4].

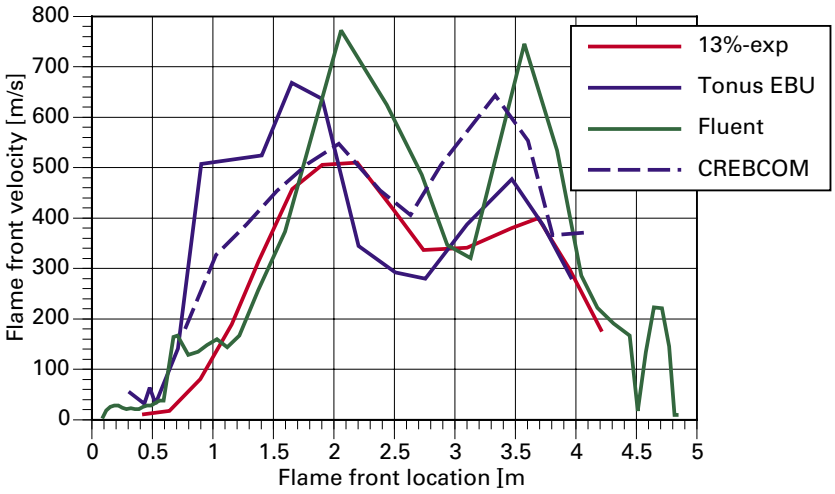

Figure 30. Flame speed comparison between FLUENT, TONUS EBU and TONUS 3D CREBCOM simulations and the uniform mixture experiment.

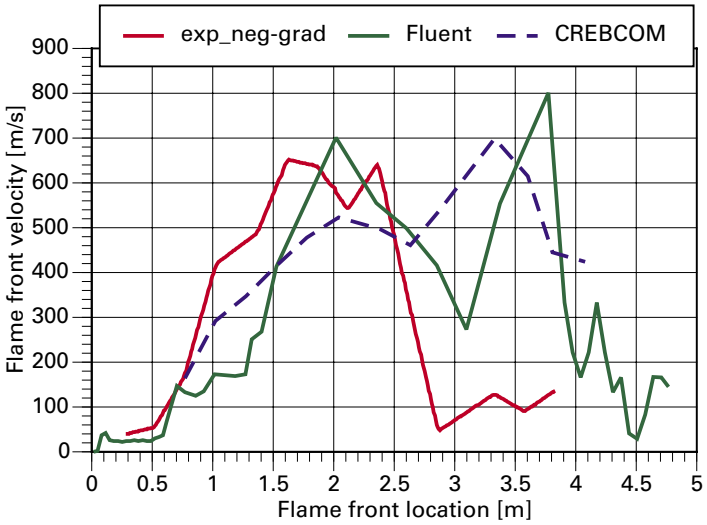

Figure 31. Flame speed comparison between FLUENT, TONUS EBU and TONUS 3D CREBCOM simulations and the negative mixture gradient experiment.

In the positive gradient case the calculation exaggerates the acceleration in the tube section. The predicted peak velocity is higher than the experimental value. Fluent gives the highest peak values. Between 2.7 m and 3.2 m the acceleration is also considerably stronger than in the experiment.

Pressure development for the uniform mixture test case is shown in Figure 33. The pressure is measured at monitor point PZT5 showing the highest pressure in most cases. In Figure 33 the pressure curve of the CREBCOM case has been shifted 0.025 s right and TONUS EBU curve 20 ms left along the time axis in order to make the values of pressure easier to compare. This is necessary because the pressure peaks do not occur at the same time in the different cases since the ignition modelling is not accurate and the ignition phase takes a relatively long time in the turbulence simulations, contrary to the CREBCOM simulations. The FLUENT curve has its original time position on the time axis. The pressure peaks observed in the FLUENT and CREBCOM 3D results are of the same magnitude. The TONUS Eddy Break-up calculation shows a significantly smaller initial pressure peak even though the flame velocity during the first acceleration reaches approximately the same value as in the FLUENT 3D case.

In Figure 30 it can be seen that the acceleration in the acceleration tube is relatively well captured by the FLUENT and TONUS CREBCOM models. However, in the tested TONUS EBU case the flame accelerates very quickly when it enters the obstacle section to a slightly exaggerated maximum speed. It is possible that this is due to the initial turbulence parameters set in the flow field and the ignition zone.

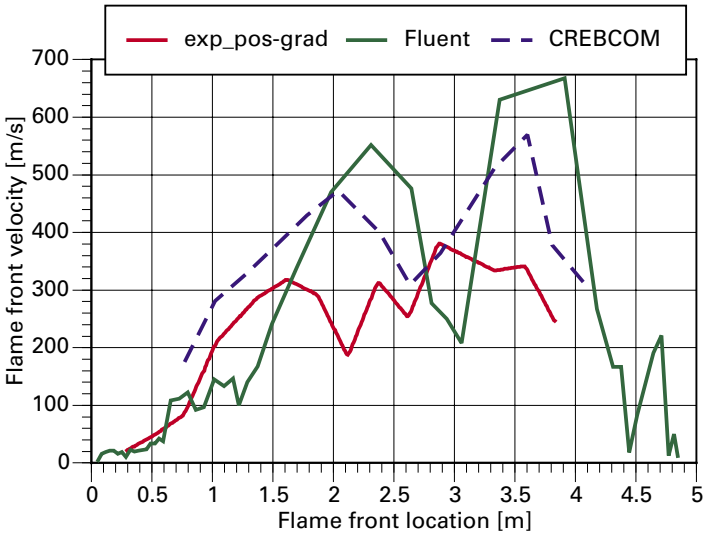

Figure 32. Flame speed comparison between FLUENT, TONUS EBU and TONUS 3D CREBCOM simulations and the positive mixture gradient experiment.

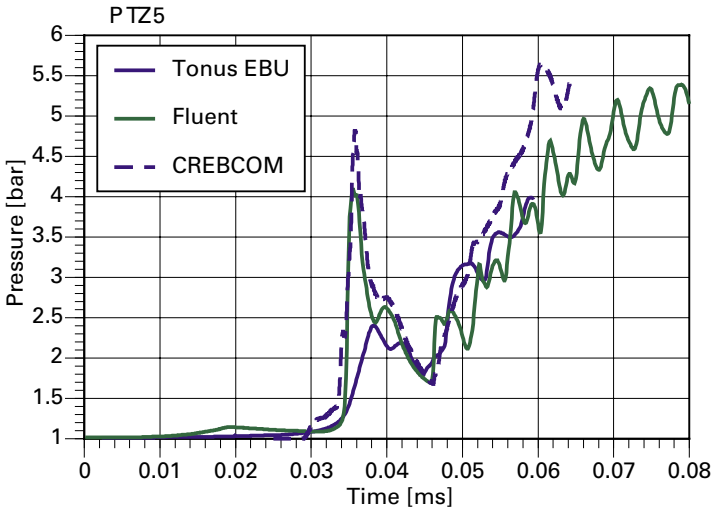

Figure 33. A pressure comparison between FLUENT, TONUS EBU and TONUS 3D CREBCOM simulations at transducer PZT5.

Table 3. Model and result summary.

TEST CASE	Models and codes	Model type	K_0 [m/s]	Peak pressure [kPa]	Maximum flame speed [m/s]
Uniform	CREBCOM	3D	10.50	484	550
	TONUS EBU	2D	–	274	670
	FLUENT EBU	3D	–	475	770
	Experiment	–	–	not reported	510
Negative	CREBCOM	3D	8.00	473	523
	FLUENT EBU	3D	–	456	700
	Experiment	–	–	not reported	650
Positive	CREBCOM	3D	4.00	356	570
	CREBCOM	2D	4.00	221	493
	FLUENT EBU	3D	–	416	660
	Experiment	–	–	not reported	380

The cases, the used models and results presented in this report are summarized in Table 3. In the case of uniform mixture and negative concentration gradient the maximum flame speeds are those measured in the acceleration tube. Instead, in the positive concentration gradient case in which the flame speed in the test is at its maximum in the dome, where the hydrogen concentration is highest, the value for the second peak is given. The given maximum pressure is the pressure of the first compression wave in the acceleration tube. The level of the final pressure into which the system "stabilizes" after the combustion in each test is about the same or slightly higher than the maximum pressure of the first compression wave of the test in question (see pressure curves in Sections 6.1 and 6.2).

7 Validation of results

7.1 Combustion models

Two different approaches to model combustion have been used. In the CREBCOM model the species diffusion and thermal conduction are not directly modelled, instead their effect is integrated into an experimental source term in the Euler equations. The model development has focused on estimating conservative pressure loads resulting from different modes of combustion. This model is computationally less expensive than the more sophisticated Eddy Break-up model in which turbulent mixing determines the combustion rate. However, the CREBCOM model performance depends on the parameter K_0 which may be difficult to estimate in some cases. Being more recently developed, the CREBCOM model has not been as comprehensively validated as the Eddy Break-up model.

In this study, a constant K_0 was used for all the cases even though the combustion rate and flame speeds depend on the hydrogen volume fraction in the combustible mixture. Implementing a non-constant value depending on the hydrogen fraction would give more accurate results than constant values based on the average fuel concentration. However, introducing a non-constant K_0 is beyond the scope of this study. For non-homogenous cases, it is also possible to use a constant value which corresponds to the maximum hydrogen volume fraction in the system in order to obtain conservative estimations for pressures and flame speeds. The validation of this method also requires further modelling.

7.2 Codes and simulation set-up

In comparing the result obtained by TONUS and FLUENT several uncertainties must be taken into account. Firstly, the computational grids are not exactly similar in the two codes since it was not possible to export and import the grids between the codes. The average cell dimension is approximately the same in FLUENT 3D grid and the fine TONUS 2D grid. The 3D grid used in TONUS represents a quarter of the geometry and it is coarser than the FLUENT grid. Secondly, different methods of extracting data of the flame positions and speeds have been used. In FLUENT the flame front has been tracked by observing which computational cell at the facility axis has the maximum reaction rate. In TONUS the reaction zone is tracked based on hydrogen mass fraction. Since the amount of measurement locations for position is the same as the amount of transducers in the tests, the accuracy of the flame speed in the simulation results corresponds to the accuracy of test results. In addition, slightly different methods of specifying the initial hydrogen concentration in the positive and negative gradient cases have been used in TONUS and FLUENT: in TONUS the initial volume fraction is taken as a linear approximation of the experimental values (the linear fit in Figure 3) while in FLUENT the initial distribution is interpolated between the test points (the fraction lines in Figure 3).

A drawback of the current version of TONUS is that the implementation of the turbulent combustion model is still under development and k-ε model is not available in 3D. This causes problems in modelling geometries with a rotational symmetry such as ENACCEF. The 2D models presented in the report do not actually represent cylinders since the axis must be defined as a slip wall. No separate "axis" boundary, such as in FLUENT, is available in TONUS for 2D models. This should be taken into account when viewing all the 2D results in this report. In this case the FLUENT results also show that the flame possibly propagates along the walls in the upper part of the acceleration tube.

This indicates that the walls and wall treatment in this test could play an important role, and due to the lack of wall treatment in TONUS the code may not be capable of capturing the shape of the flame front realistically.

The ENACCEF facility is a small-scale test facility in which it might be possible that the walls affect the behaviour of the non-homogenous mixture. A comparison to large-scale test facility data could give a more realistic evaluation of the suitability of the code for full-scale containment analysis.

8 Conclusions

The CREBCOM simulation of the uniform mixture concentration case captures the flame acceleration in the acceleration tube qualitatively well. In the positive gradient case the flame velocity in the acceleration tube is exaggerated. In the negative concentration case this acceleration is underestimated which indicates that the present value for the key parameter K_0 is too small in the acceleration tube section of the facility. The acceleration at the entrance to the dome is overestimated in all the CREBCOM calculations.

The reasonably good agreement with the test results in the uniform mixture case shows that the correlation for evaluating K0 in turbulent deflagrations is accurate enough for predicting flame speeds in this type of a closed volume. For the non-homogenous hydrogen concentration cases, a detailed simulation of the process requires re-evaluation and possibly the use of a non-constant K_0. It is noteworthy that the evaluation of K_0 based on average hydrogen concentration for the gradient cases is not feasible. Even the value K_0 = 4.0 m/s in the positive concentration case gives exaggerated flame speeds while the analytically computed value is approximately K_0 = 8 m/s which in this case is more appropriate for the negative case with lower average hydrogen volume fraction.

The results of k-ε and Eddy Break-up model using TONUS display somewhat higher maximum flame speeds than the FLUENT and CREBCOM 3D results in all the cases. The pressure behaviour is similar in the FLUENT and TONUS CREBCOM cases with the peak pressure being slightly higher in the FLUENT results. However, the peak pressure of the first pressure wave in the TONUS 2D case calculated using the EBU model differs from all the 3D cases. The pressure increase to the final pressure of the process, when no heat losses are accounted for, shows a similar oscillatory behaviour in all the cases.

A particular feature in the FLUENT simulation is that in the upper part of the acceleration tube where no obstacles are present the combustion propagates quickly next to the walls. It is concluded that this is because of the enhanced turbulence caused by wall friction in the model. Wall friction is neglected in the TONUS EBU simulation and no such effect is seen in TONUS. Based on this, it cannot be concluded how the flame behaves in reality.

The development and validation of the turbulence models in TONUS is not yet complete and some features available in FLUENT are lacking in TONUS. There are also practical differences in the performance of the codes. At the moment it is suggested to use FLUENT for containment analysis if turbulent flow and combustion should be solved in detail. However, the CREBCOM model which is not available in FLUENT is computationally less expensive and capable for reasonably accurate analysis of flame speeds, providing that a suitable K_0 is found which may be difficult in some cases.

References

[1] Beccantini, A. Implementation of CREBCOM combustion model in TONUS code. Technical Report DM2S, SFME/LTMF/RT/01-017/A (2001).

[2] Beccantini, A., Kudriakov, S. Modelling of Hydrogen Combustion in TONUS V2006.1. Technical Report DM2S, SFME/LTMF/RT/06-027/A (2006).

[3] Bentaïb, A. Specification of ENACCEF benchmark exercise relative to hydrogen combustion. Draft. Reference SARNET Document: SARNET – xxx – Revision: 0. IRSN Fontenay-aux-Roses, France, 2006. 13p.

[4] Bentaïb, A., Bleyer, A., Charlet, A., Malet, F., Djebaili-Chaumeix, N., Cheikhvarat, H., Paillard, C.E.. Experimental and numerical study of flame propagation with hydrogen gradient in a vertical facility: ENACCEF. Containment Topics-Paper No 5. The First European Review Meeting on Severe Accident Research ERMSAR-2005, Aix-en-Provence, France, 14–16 November 2005. 13p.

[5] Cant, R.S, Bray, K.N.N. A Theoretical Model of Premixed Turbulent Combustion in Closed Vessels. 1989. Combustion and Flame, 76, pp.243–263.

[6] Dorofeev, S., Redlinger, R. Description of FLAME3D. 2003. Internal report. Forschungszentrum Karlsruhe -IKET, Karlsruhe.

[7] Efimenko, A.A., Dorofeev, S.B. CREBCOM code system for description of gaseous combustion. 2001. Journal of Loss Prevention in the Process Industries 14 (2001), pp. 575–581.

[8] Lautkaski, R. Deflagration to detonation transition. Project report PRO1/P1025/05, 17.5.2005. VTT Technical research centre of Finland, Espoo 2005. 43p.

[9] Magnussen, B.F., Hjertager, B.H. On mathematical models of turbulent combustion with special emphasis on soot formation and combustion. *16th International Symposium on Combustion.* The Combustion Institute, 1976.

[10] Malet, F. Etude expérimentale et numérique de la propagation de flammes prémélangées turbulentes dans une atmosphère pauvre en hydrogène et humide. Thèse de doctorat de l'université d'Orléans. Cinétique chimique appliqué. Orleans, France, 2005. 147p.

[11] Pailhories, P. Bilan des calculs de combustion multi-D réalisés avec le modele CREBCOM du code TONUS. Note technique IRSN/DSR, (2003).

[12] Spalding, D.B. Mixed and Chemical Reaction in Steady Confined Turbulent Flames. 1971. The Combustion Institute, Pittsburgh. Proceedings of 13th International Symposium on Combustion.